

Supporting Information

Magnetorheological elastomers enabled high sensitive self-powered tribo-sensor for magnetic field detecting

Song Qi^{a,†}, Hengyu Guo^{b,c,†}, Jie Chen^b, Jie Fu^a, Chenguo Hu^{b,*}, Miao Yu^{a,*} and Zhong Lin Wang^{c,*}

a. Key Lab for Optoelectronic Technology and Systems, Ministry of Education, College of Optoelectronic Engineering, Chongqing University, Chongqing, 400044, P. R. China..

b. Department of Applied Physics, Chongqing University, Chongqing, 400044, P. R. China..

c. Beijing Institute of Nanoenergy and Nanosystems, Chinese Academy of Sciences; National Center for Nanoscience and Technology (NCNST), Beijing, 100083, P. R. China.

† These authors contributed equally to this work.

** Corresponding author. Miao Yu, E-mail: yumiao@cqu.edu.cn; Chenguo Hu, E-mail: hucg@cqu.edu.cn; Zhong Lin Wang, E-mail: zhong.wang@mse.gatech.edu.*

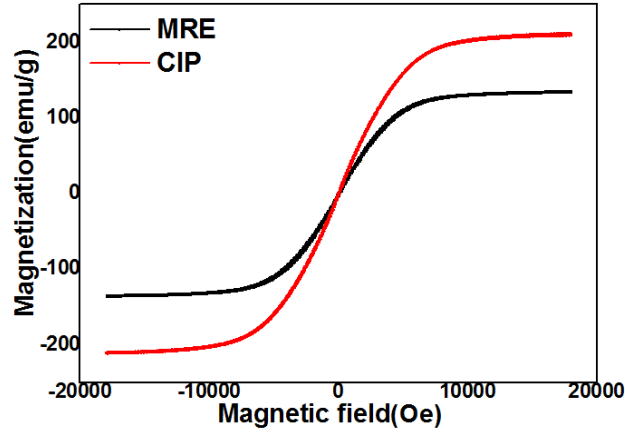


Fig. S1 Magnetization curves (magnetic moment per unit mass) of CIPs and 60wt%-MRE.

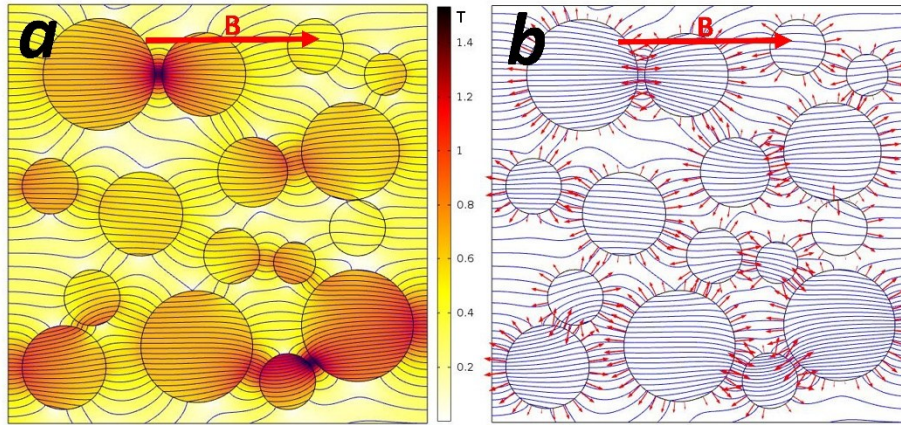


Fig. S2 Magnetic simulation of representative volume element (RVE) of MRE evaluated by COMSOL.

(a) Magnetic flux density indicated by the color and streamline; (b) Magnetic surface stress tensor indicated by the red arrow on the particle surface.

Note S2. The qualitative fitting analysis of the magnetic-induced deformation of MRE film

Fig.S3 shows the deformation diagram of the MRE film, we assume that the deformed MRE film formed a cone, the radius of MRE film is R , from Eq.(6) we can deduce that the Δd of particle can be expressed as

$$\Delta d = \frac{2\pi\mu_0 r^6 H^2}{d^4 k} \quad (S1)$$

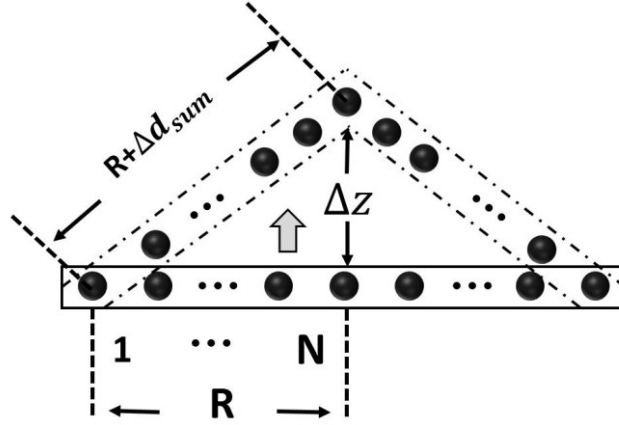


Fig. S3 The schematic diagram of the simplified deformation of the MRE film.

To simplify, we only consider a single-layer particles, as a consequence, the total Δd can be expressed as

$$\Delta d_{sum} = \sum_{n=1}^N \Delta d_n = \sum_{n=1}^N \frac{2\pi\mu_0 r^6 H^2}{d^4 k_n} \quad (S2)$$

k_n is the coupling constant between the different particles, the value of Δd can be positive or negative, and the sign of Δd indicated the F'_{el} is a tensile or compressive elastic force. Eq (S2) can be simplified to

$$\Delta d_{sum} = KH^2 \quad (S3)$$

where $K = \sum_{n=1}^N \frac{2\pi\mu_0 r^6}{d^4 k_n}$ is assumed as constant. Therefore, the deformation along the Z-axis direction of center in MRE film can be expressed as

$$\Delta z = \sqrt{(R + \Delta d_{sum})^2 - R^2} \quad (S4)$$

Simultaneous equations S3 and S4 can be obtained

$$\Delta z = \sqrt{K^2 H^4 + 2KRH^2} \quad (S5)$$

we also assume that the dielectric permeability μ is a constant, the magnetic flux density $B = \mu H$, and from Eq (2) we can deduce that the magnetic field strength $H_0 = \frac{H}{\alpha f(\lambda)+1}$, therefore the

relationship between the Δz and B can be expressed as follow

$$\Delta z = B\sqrt{\varphi B^2 + \omega} \quad (S6)$$

where $\varphi = \left(\sum_{n=1}^N \frac{2\pi\mu_0 r^6}{d^4 k_n} \right)^2 \times \frac{1}{[(\alpha f(\lambda)+1)\mu]^4}$ and $\omega = \frac{2R}{[(\alpha f(\lambda)+1)\mu]^2} \times \left(\sum_{n=1}^N \frac{2\pi\mu_0 r^6}{d^4 k_n} \right)$ are constant.

We have detected the magnetic-induced deformation Δz of the MRE films with different CIP content by using the laser rangefinder, the test dates and the fitting result according to Eq (S6) shown in **Fig. S4**, the fitting parameters φ and ω were listed in Table S1. It can be seen that the Eq (S6) can be well used to describe the magnetic-induced deformation Δz of the MRE films. The parameters φ and ω were increased with the increasing CIP content, which indicated the MRE film with the higher CIP content has the higher magnetic-induced deformation sensitivity. It can be attributed to stronger magnetic interaction of CIP in the MRE film with higher CIP content.

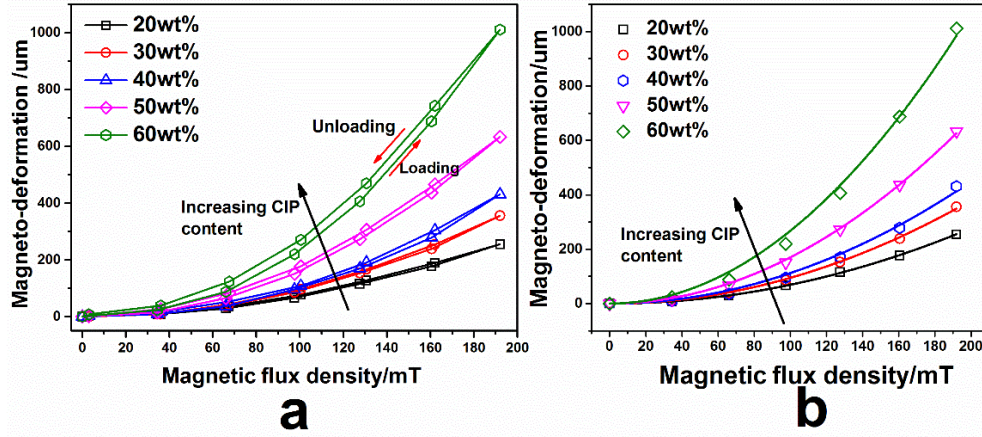


Fig. S4(a) The magnetic-induced deformation of the MRE film with different CIP content; (b)

Fitting result of the magnetic-induced deformation based on Eq (S6). (Symbols are experimental data and solid lines are the predicted curves.)

Table S1.The values of parameters of the fitting result according to Eq (S6).

Sample	$\varphi(\times 10^{-5})$	$\omega(\times 10^{-3})$
Sample-20wt%	4.79 ± 0.04	1.3 ± 0.1
Sample-30wt%	8.96 ± 0.17	5 ± 0.3
Sample-40wt%	12.53 ± 0.56	8 ± 0.5
Sample-50wt%	28.83 ± 0.48	10 ± 0.4
Sample-60wt%	71.36 ± 2.68	15 ± 0.8

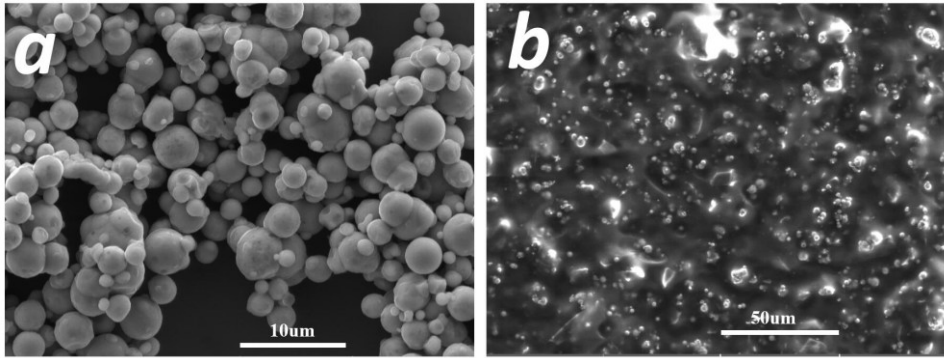


Fig. S5 SEM images of the (a) CIP and (b) isotropic MRE with 60wt% CIP.

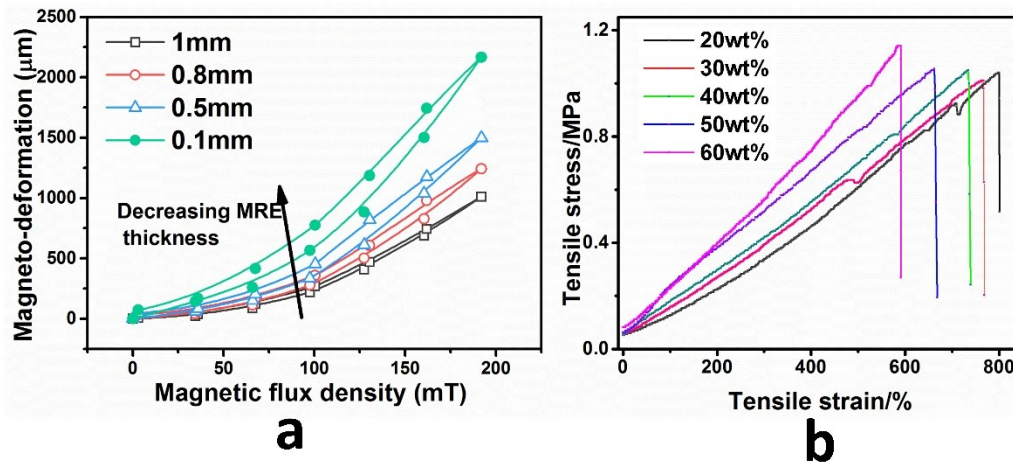


Fig. S6 (a) The magnetic-induced deformation of the MRE film with different thickness; (b) Tensile curve of the MRE film with different CIP content.

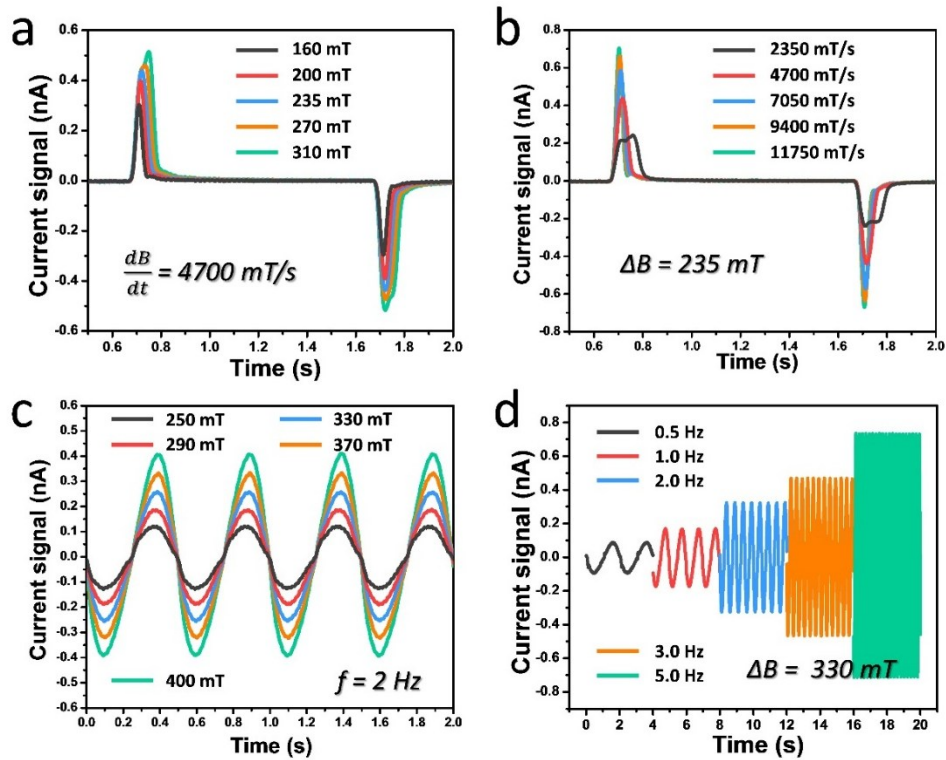


Fig. S7(a) The output current of TENG under the time-varying magnetic field, the different curves corresponding to the different changing magnitude of magnetic field; (b) The output current of TENG under the time-varying magnetic field, the different curves corresponding to the different changing rate of magnetic field; (c) The output current of TENG under the sinusoidal magnetic field with frequency of 2Hz, the the different curves corresponding to the different changing amplitude of magnetic field; (d) The output current of TENG under the sinusoidal magnetic field with amplitude of 330mT , the the different curves corresponding to the different frequency.

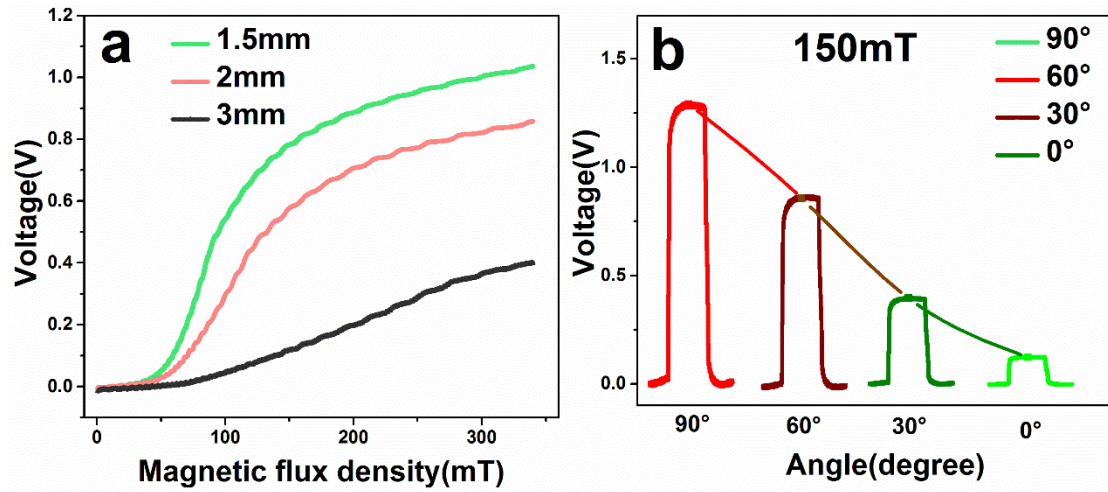


Fig. S8 (a) The output voltage of TENG under the uniformly increases UMF, the different curves corresponding to the different gap between the upper part and lower part; (b) Output voltage of TENG under the transient UMF with different angle.